LANGMUIR CIRCULATIONS IN A LABORATORY TANK

Mizuno, Shinjiro
Research Institute for Applied Mechanics, Kyushu University : Associate Professor

https://doi.org/10.5109/6781005

出版情報：Reports of Research Institute for Applied Mechanics. 31 (97), pp.47-59, 1983-09. 九州大学応用力学研究所
バージョン：
権利関係：

Reports of Research Institute for Applied Mechanics
Vol. XXXI, No. 97, 1983

LANGMUIR CIRCULATIONS IN A LABORATORY TANK

By Shinjiro MIZUNO*

Windward and lateral drift currents at the surface were measured at a node and an antinode of crossed waves to clarify the flow induced by Langmuir circulations when a wind blew over mechanically generated crossed waves. For the crossed wave without the wind action, the Lagrangian surface current ageed well with the Stokes drift. For the wind and crossed wave coexistent case, the wind-induced drift, or total drift minus Stokes wave drift, was 0.7-0.8 times as much as that of the wind-only case. The lateral drift measured close to a node was about 0.8 % of the mean wind speed, while no lateral drift close to an antinode. When the eddy viscocity is assumed to be 1 cm^2/sec, the experimental results of the lateral surface drift agree, but those of the windward surface drift do not agree, with the Craik and Leibovich theory. The reason for the disagreement may be that most of the wind-induced windward drift is directly driven by the wind stress.

Key words :Langmuir circulations, wave-current interaction, surface drift current.

1. Introduction

Many mechanisms have so far been proposed, as discussed by Scott *et al*[1], to explain the Langmuir circulations and their associated wind streaks. From the observations of the Langmuir circulations in lakes and in oceans, Gordon[2], Myer[3], and others pointed out that surface wave action, above all, played an important role in their generation. In relation to these observations, two noticeable theories based on wave-current interactions appeared almost at the same time. One is Garrett theory[4], which is based on the interaction between the Stokes transport of surface waves and horizontal current shear. According to his theory, the convergence of surface flow due to the organized motion corresponds to maxima of lateral profile of windward surface current. The other is Craik and Leibovich theory[5], which is referred to as CL1 hereafter. In this theory the Langmuir circulations are directly driven by the interaction between current shear and the crossed waves propagating at angles with respect to the wind. It was later extended to include an instability mechanism (for more

* Associate Professor, Research Institute for Applied Mechanics, Kyushu University.

details, see Leibovich[6]). One of the most noticeable results of the theory is that the wind streaks appear along the nodal lines of crossed waves when both the wind and the crossed waves are present.

These recent theories have attracted wide attention to the problem of Langmuir circulations. Nevertheless, there are very few experimental studies that have examined the validity of these theories. Faller[7] first found the existence of steady Langmuir circulations in a laboratory tank in which wind blew gently over regular crossing waves. The observed circulations were in general agreement with the CL1 model. Faller and Cartwright[8] examined the motions of surface floats in the transition stage of the formation of Langmuir circulations after the onset of crossed wave in the wind field.

In this study we attempt to measure Lagrangian surface current induced by the Langmuir circulations that are formed when mechanically generated crossed waves and wind are present. First, Faller's results suggesting the validity of CL 1 model are also confirmed in our experimental facility by the method of visualization. Second, we present the experimental results of surface windward and lateral drift currents measured after steady Langmuir cells have been established. The windward surface drift current is obtained for the following three cases : wind-only, mechanically generated crossed wave-only, and the coexistent case of the wind and the crossed wave, while the lateral drift is obtained for the third case only. Measurements of subsurface current are to be made in the near future.

2. Experimental apparatus and procedure

The experiments were made in a rectangular wave tank, 70 m long, 8 m wide, and 3 m deep, at Tsuyazaki laboratory, Kyushu University. Figure 1 shows a general layout of the wind-wave tank that is equipped with a row of 8 equally divided, independently operative plungers, which generate a pair of crossed waves

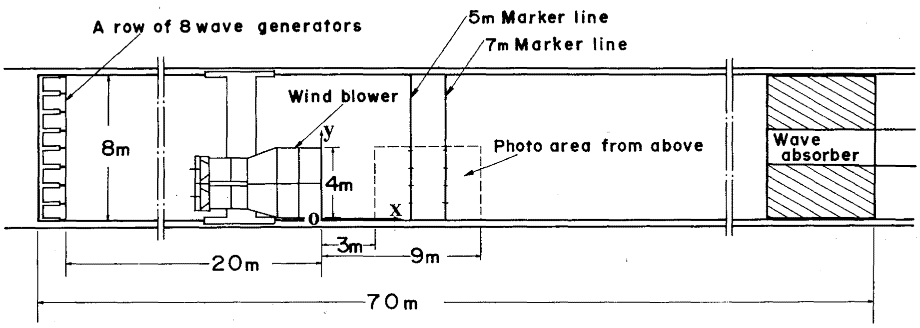

Figure 1 A schematic diagram of the wind-wave tank.

propagating at angles $\pm\alpha$ to the wind direction and produce alternate nodal and antinodal lines aligned parallel to the wind direction. Then the water surface displacement η is expressed as

$$\eta = 2a \cos\left(\varkappa\sqrt{1-\left(\frac{n\pi}{\varkappa D}\right)^2}\,x - \omega t\right)\cos\left(\frac{n\pi}{D}y\right), \tag{1}$$

where a, $\varkappa$, and ω are amplitude, wavenumber, and angular frequency of a monochromatic wave train, respectively ; n is the number of nodal lines, D the width of the tank, x the windward distance measured from the wind blower, y the spanwise distance measured from one side wall of the tank (see Fig. 1), z positive upward, and t the time. Then, $n\pi/\varkappa D$ is related to α by $\sin\alpha = n\pi/\varkappa D$, the wave period is given by $T = 2\pi/\omega$, and the wave slope in the x-direction by $a\varkappa\cos\alpha$. The Stokes wave drift on the surface corresponding to (1) is

$$U_S = 2\omega a^2\varkappa\cos\alpha\left[1+\cos^2\alpha\cos\left(\frac{2n\pi}{D}y\right)\right]. \tag{2}$$

The wind blower is an open jet type, 4 m wide and 40 cm high in the outlet. It was fixed to one side wall of the tank 20 m downstream of the row of the plungers, as shown in figure 1. The bottom of the wind blower was 25 cm above the water surface to maintain sufficient clearance for the passage of mechanically generated waves.

The experiments consist of the visualization of flow patterns on the water surface and the measurements of surface drift currents. The wind and wave parameters used in the experiments are summarized in Table 1.

Table 1 Wind and wave parameters used in the experiments of surface drift current, where $2a\varkappa\cos\alpha$ represents wave steepness at an antinode, W wind speed, and refer to the text for the definition of the other parameters.

n	T(sec)	a(cm)	$\varkappa$(cm^{-1})	α(°)	$2a\varkappa\cos\alpha$	W(m/s)	u_*(cm/s)
5	1.1	3.75	$2\pi/189$	36	0.2	4.5	0.7

Small white polyetyren spheres of 0.2 to 1 mm in diameter were used as surface floats for the visualization. Two kinds of flow patterns were obtained by scattering them on the surface : steady and unsteady patterns. To obtain the former they were scattered continuously during the experiments and uniformly in the lateral direction just downwind from the outlet of the wind blower. To obtain the latter, they were uniformly scattered before the experiments inside an open, rectangular wooden frame (40 cm wide and 4 m long), which were floated on the surface with long sides in the lateral direction at $x = 3$ m. Just before arrival of the mechanical waves the wooden frame was removed from the surface and the floats drifted on the surface. The photographs of drifting floats were taken at every 5 seconds for 2 minutes after their release from the above and upstream locations.

Surface drift currents U in the wind direction were obtained at two y-positions corresponding to an antinode ($y = 1.6$ m) and a node ($y = 2.4$ m) of the mechanical waves for the following three cases : wind-only case, mechanical wave-only case, and the coexistent case of the wind and wave, by measuring the time interval during which a very small piece of punched cards (1 mm× 3 mm) passed two marker lines ($x = 5$ and 7 m, cf. Fig. 1). The lateral surface currents V were measured only for the third case. To measure V a number of thread lines were arranged at equal interval of 10 cm parallel to nodal lines of the mechanical waves. It was then obtained by measuring the time interval during which a surface float passed two thread lines 20 cm apart in the lateral direction.

3. Experimental results

Wind and wave characteristics

Figures 2 and 3 show the longitudinal and lateral distributions of mean wind speed, which were measured at $y = 2$ m for the x-distribution and at $x = 6$ m for the y-distribution at a height of 15 cm. These figures indicate that the wind field is approximately uniform over a rectangular area which is 3 to 12 m downwind of the wind blower and 4 m wide from one sidewall. Figure 4 shows the spanwise distributions of the peak to peak wave height measured at $x = 6$ m with and without the wind in the presence of the mechanical waves. We can see that the formation of regular short-crested waves is fairly well realized across the tank, although the locations of node tend to shift slightly to the right when the wind blows.

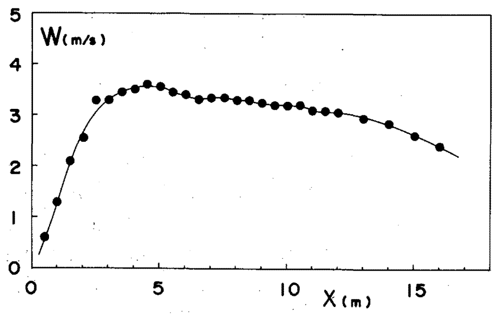

Figure 2 Longitudinal distribution of mean wind speed at a height of 15 cm and at $y = 2$ m.

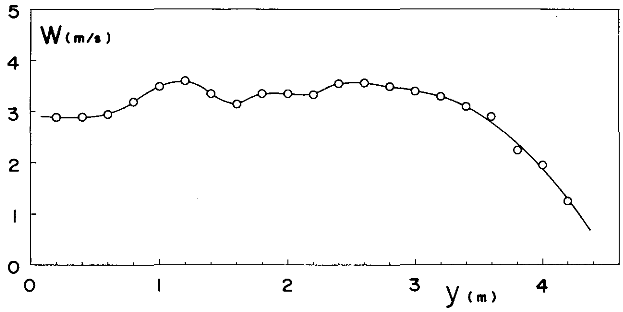

Figure 3 Lateral distribution of mean wind speed at a height of 15 cm and at $x = 6$ m.

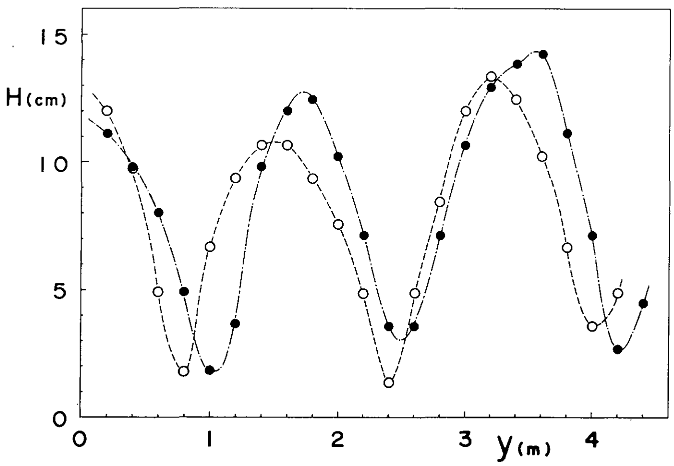

Figure 4 Lateral distributions of peak to peak wave height, H, at $x = 6$ m in the presence of mechanical waves : o, without wind ; ●, with wind (W = 3.4 m/s). Note that 5 nodal lines are given by $y = 0.8$, 2.4, 4.0, 5.6, and 7.2 m.

Visualization experiments

Photo 1a and 1b show the time sequence of the movement of the surface floats after their release without and with the wind, respectively. When there was no wind, the movement of the floats clearly indicated a typical pattern of the Stokes wave drift (Eq. 2) that moved faster at antinodes than at nodes. When the wind blew the floats converged rapidly toward the nodal lines of the mechanical waves. As a result, steady Langmuir cell patterns appeared approximately 40

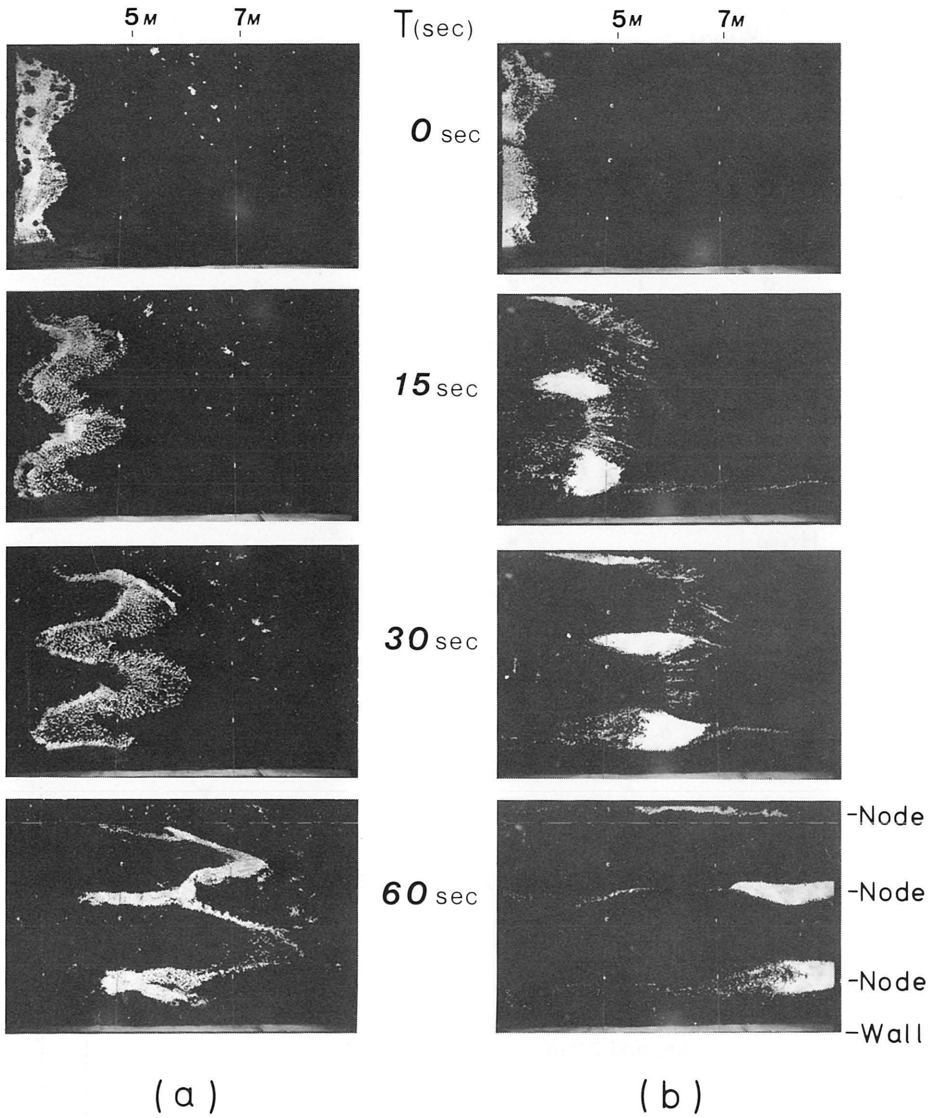

Photo 1 Time sequences of surface float patterns produced by the mechanical waves only (a), and by an interaction between the wind and waves (b). Wind and waves come from left. White marks are attached to 5 m and 7 m lines every 1 m from the wall.

seconds after an arrival of the mechanical waves. Photo 2 shows the steady windrows aligned along the nodal lines parallel to the wind, which agree qualitatively with those predicted by Craik and Leibovich[5]. The similar results were obtained by Faller[7] under the lighter wind and the crossed waves of smaller amplitude. The present results confirm Faller's finding independently.

Steady surface drift current experiments

The experimental results of the windward surface drift currents for the three cases are summarized in Table 2, where each value represents the average and the probable error of more than 5 measurements. In these experiments a refer-

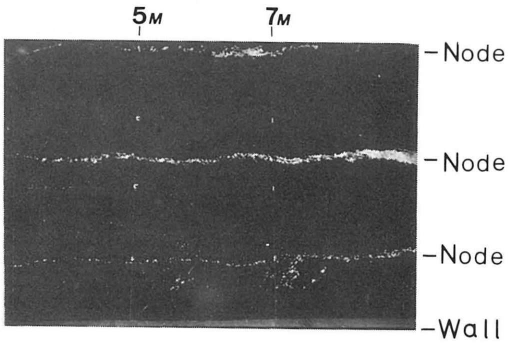

(a)

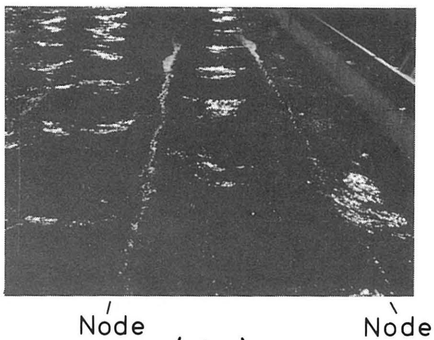

(b)

Photo 2 Surface float patterns illustrating steady Langmuir circulations, taken approximately 2 minutes after the arrival of the mechanical waves at $W = 3.4$ m/s : (a), top view ; (b), upstream view.

ence wind speed was 4.5 m/s, which was measured at $x = 10$ m, $y = 2$ m, and $z = 15$ cm. The wind friction velocity was determined from the logarithmic law of the mean wind speed near the surface, and the water friction velocity u_* in Table 1 was estimated by equating the wind and water stress. Table 2 indicates that for the wind-only case the surface drift currents are about 4.3 % of the reference wind seed, and that the measured Stokes wave drift currents of the mechanical wave agree very well with the theoretical values (Eq. 2), which yield 7.1 cm/s at an antinode and 1.5 cm/s at a node. A good agreement between them suggests that the formation of the short-crested waves is fully satisfactory.

Table 2 Results of windward surface drift current for three different wind and wave conditions.

	U(cm/s)	
	Y=240cm (node)	Y=160cm (antinode)
wind drift (no crossed wave)	18.9±0.3	20.7±0.3
Stokes wave drift (no wind)	1.2±0.1	7.9±0.2
Total drift (wind+crossed wave)	16.3±0.1	21.8±0.8

For the wind and wave coexistent case, there is a noticeable experimental fact ; that is, the measured surface drift currents, which are called total surface drift, are considerably less than the sum of the wind-only and the mechanical wave-only cases. In particular, note that the total surface drift at the node is over 2 cm/s smaller than that of the wind-only case. If the difference between the total surface drift and the Stokes wave drift is interpreted after Wu[9] as the wind-induced drift in the presence of the mechanical waves, then it yields

$$U_W = 15.1 \pm 0.2 \text{ cm/s} \quad \text{at the node,}$$
$$U_W = 13.9 \pm 1.0 \text{ cm/s} \quad \text{at the antinode.}$$

Thus the values of the wind-induced drifts at the node and at the antinode in the presence of the mechanical waves are approximately 0.8 and 0.7 times as much as those in the absence of the mechanical waves, respectively.

Table 3 shows the lateral surface currents measured at several lateral locations close to the node ($y = 2.4$ m) under the same wind and wave conditions as for the windward drift, where each current value represents the average and the probable error of more than 5 measurements. It is clear from Table 3 that the lateral surface current near the node coverges toward the node with the maximum speed of 3-4 cm/s or about 0.8 % of the reference wind speed. On the other

Table 3 Results of lateral surface current measured close to a node (y = 240 cm) as a function of y-coordinates. Note that the sign of V is reverse between 240 and 250 cm.

y-coordinates (cm) of measured section	V(cm/s)
210 – 230	3.3 ± 0.5
220 – 240	2.9 ± 0.6
250 – 270	−3.3 ± 0.4
260 – 280	−4.1 ± 0.2

hand, the measurements of the lateral current close to the antinode (y = 160 cm) were very difficult and actually impossible, though attempted, because an individual float moved diversely without showing any tendency of either divergence or convergence.

4. Discussions

According to the Pollard's review[10], the Langmuir circulations in the field observations usually do not exist in winds less than 3 m/s. The windrows similar to Photo 2, however, formed from very low wind speed less than 3 m/s to high wind speed when the wind and the crossed waves were present. They also occurred even under a very strong stable stratification with the surface and bottom temperature difference of about 9°C in a depth of 3 m. That is, they seem to be found over a wider range of experimental conditions than expected, if wind and crossed wave exist at the same time.

Leibovich[11] and Leibovich and Radhakrishnan[12] obtained several numerical solutions for the drift currents and Langmuir circulation system produced according to the CL1 mechanism. The velocity vector of the organized motion is given by

$$\mathbf{V} = (u_*^2/\nu_T \mathrm{k})(u,0,0)+(u_* a/\nu_T)^{\frac{1}{2}}(0,v,w), \tag{3}$$

where ν_t is an eddy viscosity that is assumed to be constant, and u, v, and w are the dimensionless velocity components that were solved numerically for two different wave angles. Although the estimated value of ν_t is necessary to compare with the present results, we cannot estimate it from the present data of the surface drift current alone. So in this paper we assume that ν_t is 1 cm^2/sec, which is not always unreasonable because Leibovich and Radhakrishnan[12] estimated (in Eq. 22 of their paper) that

$$\nu_T \approx 1.1\times 10^{-2} a^2 \omega, \tag{4}$$

which gives 0.9 cm^2/sec for the present wave parameters(Table 1).

When $\nu_t = 1\ \mathrm{cm^2/sec}$, the characteristic parameters of the CL1 model corresponding to the present experimental conditions are as follows : $u_*^2/\nu_T \chi = 14.8$ cm/s, $u_* a(\omega/\nu_T)^{\frac{1}{2}} = 5.8$ cm/s, $T_d = 4.8$ sec, and $La = 5.3\times10^3$, where T_d represents the characteristic time scale of the Langmuir circulations and L_a, which is called Langmuir number, the dimensionless number interpretable as an inverse Reynolds number. According to Leibovich[11], the formation time of the well-developed Langmuir circulations obtained from the numerical calculation is about 10 T_d, while the one determined from the time sequence of Fig. 7 (b) was 40 sec or 8 T_d. By using the above parameters and the numerical solutions for the wave angle $\alpha = 30°$, the theoretical values of the surface drifts are calculated and compared with the present results in Table 4.

Table 4 A comparison of the present results of surface drift current with the CL1 theory, where ν_t is assumed to be 1 cm²/sec in the estimation of the theoretical values.

		Us	U_W	$Ut \equiv Us + U_W$	W_{max}	V_{max}
Theory	node	1.5	6	7.5	−4	4
	antinode	7.1	4	11.1	2	
Experiment	node	1.2	15.1	16.3	—	3~4
	antinode	7.9	13.9	21.8	—	

A good agreement is found between the theoretical and the experimental values for the lateral velocity only, which shows that ν_t must be of the order of 1 cm²/sec for V to be consistent with the CL1 theory. For the windward surface drift component, however, there is a great discrepancy between them. That is, the experimental values U_W are over two times as large as the corresponding numerical solutions. This is probably because the surface current other than the Langmuir circulations contributes to U_W. Although Craik and Leibovich[5] assumed that the total surface current consisted of the sum of the Stokes wave drift and the convection-induced drift, it is well known (e. g., Wu[9]) that the windward current is primarily driven by the wind friction in a short fetch. It is therefore reasonable to assume that the wind-induced drift defined in Section 3(U_W) consists of the convection-induced drift (U_c) and the wind-directly-driven drift (U_{Wd}), i. e.,

$$U_W = U_c + U_{Wd}.$$

If the convection-induced drift is given by the numerical solutions of the CL1 theory, the wind-directly-driven drift is as follows :

$U_{Wd} \sim 10$ cm/s at the node,
$U_{Wd} \sim 9$ cm/s at the antinode.

That is, we find that most of the wind-induced drift is directly driven by the wind stress *rather than* the Langmuir circulations in the present experiment.

Finally, let us consider why the wind-induced drift should decrease with an addition of the mechanical waves. There seem to be at least two reasons : (1) the reduction of wind speed by the presence of the mechanical waves, or (2) the wave-current interactions including the Langmuir circulations. In order to examine the wind effect, the measurements of the mean wind speed with and without the mechanical waves were made at several heights (8, 16, and 25 cm above the mean surface) of the node and antinode under the same wind condition, and yet no significant change of the wind speed was found by the presence of the waves. However, we do not examine how the wind profile changes very near the surface. In order to check the wave-current interaction, the knowledge of subsurface currents is required. Since the measurements of subsurface current are not made in this study, it is difficult to discuss the wave-current interaction in detail. Here we only point out two kinds of wave-current interaction, both of which would be able to reduce the surface drift below the wind-only case. One mechanism is Langmuir circulations, whose convection action, as pointed out by Faller and Cartwright[8)], would certainly reduce the surface drift. Another mechanism is breaking of wind-generated waves by the presence of the longer crossed waves. Mitsuyasu[13)] and Phillips and Banner[14)] found that wind-generated short waves, superposed on longer mechanically generated waves, reduced the maximum amplitude that the short waves could attain with increasing the steepness of the longer waves. For example, it is reported that when the long-wave steepness was 0.175, the short waves disappeared into the noise level. Phillips and Banner[14)] pointed out that this was due to the short wave breaking near the crest of the longer waves. In the present experiment the maximum slope of the crossed waves is 0.2 at the antinode as shown in Table 1. The breaking of wind-generated waves therefore may occur more actively near the antinodes of the crossed waves, which would increase the energy of turbulent motion to bring about vigorous vertical mixing through the upper layer. Thus the turbulent mixing associated with the wave breaking would cause high momentum of the near-surface current to diffuse downward.

Faller and Cartwright[8)] made similar experiments, in which they followed unsteady motions of many surface tracers after the onset of crossed waves under a wind action by taking the pictures with a 16 mm movie camera. Surface velocity components of all tracers were subjected to a least-square Fourier analysis in a lateral coordinate to determine the first few Fourier coeficients. There are many differences between the present and their experimental conditions. The greatest difference is that in the present experiments the motion of floats was followed at or close to the antinode and node under steady wind and wave conditions, while they analyzed unsteady motions of surface floats as a function of the time relative to the passage of the wave front. Nevertheless, we would like to point out that there are many common points between both the experimental results. That is, they also found that by adding the crossed wave to the wind field the wind-induced drift decreased with time, except short time after the onset of the wave. Secondly, the lateral surface drift converged toward the nodal lines for the case that the wind direction was in the same direction with the propagation of the crossed wave. Thirdly, the maximum lateral surface drifts that obtained by them for W = 1.39 m/s and 2.32 m/s were, respectively, about 0.4 % and 0.7 % of the reference wind velocity, which was measured at 5 cm above the surface. These values are of the same order of percentage as the present one (0.8 %).

Acknowledgements

The author wishes to thank Professor H. Mitsuyasu for his critical reading of the manuscript and valuable comments. He is also indebted to Mr. K. Marubayashi and Mr. M. Ishibashi for their assistance with the experiments and the data analysis, and to Miss M. Hojo for preparing the manuscript.

References

1) Scott, J. T., Myer, G. E., Stewart, R. & Wather, E. G. : On the mechanism of Langmuir circulations and their role in epilimnion mixing, Limnology and Oceanography ***14*** (1969) 493-503.
2) Gordon, A. L. : Vertical momentum flux accomplished by Langmuir circulations, J. Geophys. Res. ***75*** (1970) 4177-4179.
3) Myer, G. E. : Structure and mechanics of Langmuir circulations on a small inland lake. Ph. D. Dissertaion, State University of New York, Albany, 107 pp.
4) Garrett, C. J. R. : Generation of Langmuir circulations by surface waves - a feed back mechanism, J. Mar. Res. ***34*** (1976) 117-130.
5) Craik, A. D. D. & Leibovich, S. : A rational model for Langmuir circulations, J. Fluid Mech. ***73*** (1976) 401-426.
6) Leibovich, S. : The form and dynamics of Langmuir circulations, Annual Review of Fluid Mechanics **15** (1983) 391-427.
7) Faller, A. J. : Experiments with controlled Langmuir circulations, Science **201** (1978) 618-620.
8) Faller, A. J. and Cartwright, R. W. : Laboratory studies of Langmuir circulations, J. Phys. Oceanogr. **13** (1983) 329-340.
9) Wu, J. : Wind induced drift currents, J. Fluid Mech. **68** (1975) 49-70.
10) Pollard, R. T. : Observations and theories of Langmuir circulations and their role in near surface mixing. In A Voyage of Discovery, George Deacon 70th Anniversary Volume, M. Angel, ed. (Pergamon Press, 1977) 235-251.
11) Leibovich, S. : On the evolution of the system of wind drift currents and Langmuir circulation in the ocean. Part 1. Theory and the averaged current, J. Fluid Mech. **79** (1977) 715-743.

12) Leibovich, S. & Radhakrishnan, K. : On the evolution of the system of wind drift currents and Langmuir circulations in the ocean. Part 2. Structure of the Langmuir vortices, J. Fluid Mech. **80** (1977) 481-507.
13) Mitsuyasu, H. : Interactions between water waves and wind (I), Rep. Res. Inst. Appl. Mech. **XIV**, No. 48 (1966) 67-89.
14) Phillips, O. M. and Banner, M. L. : Wave breaking in the presence of wind drift and swell, J. Fluid Mech. **66** (1974).

(Received June 30, 1983)